PAPER

Check for updates

Anti-Stokes photoluminescence study on a methylammonium lead bromide nanoparticle film†

Anna Jancik Prochazkova, [ID] [a,b] Felix Mayr,[a] Katarina Gugujonovic,[a] Bekele Hailegnaw,[a] Jozef Krajcovic,[b] Yolanda Salinas, [ID] [c] Oliver Brüggemann, [ID] [c] Niyazi Serdar Sariciftci [ID] [a] and Markus C. Scharber [ID] *[a]

Photon cooling *via* anti-Stokes photoluminescence (ASPL) is a promising approach to realize all-solid-state cryo-refrigeration by photoexcitation. Photoluminescence quantum yields close to 100% and a strong coupling between phonons and excited states are required to achieve net cooling. We have studied the anti-Stokes photoluminescence of thin films of methylammonium lead bromide nanoparticles. We found that the anti-Stokes photoluminescence is thermally activated with an activation energy of ~80 meV. At room temperature the ASPL up-conversion efficiency is ~60% and it depends linearly on the excitation intensity. Our results suggest that upon further optimization of their optical properties, the investigated particles could be promising candidates for the demonstration of photon cooling in thin solid films.

Introduction

Lead halide perovskites such as hybrid organic–inorganic lead halides have emerged as novel ionic semiconductor materials. Thereby, a new generation of optoelectronic devices such as low-cost solar cells, light-emitting diodes, photodetectors and lasers is possible.[1] Simple and versatile chemical preparation procedures, composition controlled band gap engineering, outstanding electrical and optical properties (such as long charge carrier lifetime and very high photoluminescence quantum yield) have made lead halide perovskites to one of the most active research fields in material science in recent years. Progress in the synthesis allowed the preparation of colloidal perovskite nanocrystals with photoluminescence (PL) quantum yields up to 100%.[2–6] High performance nanocrystals emitting in various different colors are available today making them ideal candidates for lighting and display applications. Colloidal quantum dots are also used as imaging tools in biology and medicine and as fluorescent up- and down-converters.[7,8]

[a]*Institute of Physical Chemistry and Linz Institute of Organic Solar Cells (LIOS), Johannes Kepler University Linz, Altenbergerstrasse 69, 4040 Linz, Austria. E-mail: markus_clark.scharber@jku.at*
[b]*Institute of Chemistry and Technology of Environmental Protection, Brno University of Technology, Purkynova 464/118, 61200 Brno, Czech Republic*
[c]*Institute of Polymer Chemistry (ICP), Johannes Kepler University of Linz, Altenbergerstrasse 69, A-4040 Linz, Austria*
†Electronic supplementary information (ESI) available. See DOI: 10.1039/d0nr04545d

Luminescence up-conversion is the process whereby a system absorbs low energy photons and emits higher energy photons. The most commonly studied luminescence up-conversion mechanisms result from multi-photon processes using rare earth dopants or triplet–triplet annihilation. Alternately, single photon up-conversion, also known as anti-Stokes photoluminescence (ASPL) can occur when the energy difference between the absorbed low energy photon and the emitted high energy photon is provided by phonons. Because this process does induce phonon annihilation, taking away the lattice thermal energy by optical radiation, this phenomenon can lead to "photoinduced cooling". The possibility of using anti-Stokes photoluminescence to cool a fluorescent gas with radiation was first proposed by Pringsheim in 1929.[9] In 1946, Landau developed the theoretical basis of the process by assigning entropy to light.[10] He pointed out that the entropy of a radiation field is a function of both the solid angle of the propagating light and the frequency bandwidth. During ASPL cooling light with narrow spectral bandwidth and high directionality is converted into a broadband, isotropic luminescence, increasing entropy of the system even in the presence of local cooling. Experimentally, anti-Stokes cooling is difficult to achieve and successful cooling has first been reported in rare-earth doped glasses and a fluid solution of a laser dye.[11,12] Anti-Stokes cooling in semiconductors and quantum dots remains challenging.

The requirements to achieve anti-Stokes PL cooling in quantum dot emitters have been formulated by Rakovich *et al.*:[13]

(a) Appropriate electronic structure with ground and excited states well separated from each other in energy, with the excited state split into two closely spaced levels

Paper

(b) Strong electron–phonon and hole–phonon interactions to ensure high rate of absorption of lattice phonons

(c) High photoluminescence quantum yield in order to minimize the dissipation of photon energy through sample heating due to non-radiative transitions

(d) Independence of the emission properties of the excitation wavelength

(e) Growth of the ASPL intensity with temperature.

A three-level model illustrating the basic processes for the generation of anti-Stokes photoluminescence is shown in Fig. 1(e). After photoexcitation (0 → 1) the higher lying state 2 is populated *via* the annihilation of a phonon. Radiative recombination to the ground state (2 → 0) leads to anti-Stokes photoluminescence.

In addition, net cooling often remains elusive due to large parasitic absorption in the band tail or due to impurities. The photoluminescence quantum efficiency required for cooling depends on the band gap of the emitter and needs to be >96% for an ideal system with an emission in the visible range.[14] This explains why semiconductor structures, which can be cooled by light, are rare. Experiments on CdS nanobelts[15] and different perovskite platelets[16] suggest cooling due to anti-Stokes photoluminescence.

Many colloidal quantum dots based on perovskite semiconductor material appear to be ideal for photon cooling due to their outstanding optical properties. However, the nature of their lowest excited state, the anti-Stokes up conversion mechanism and the radiative and non-radiative recombination in
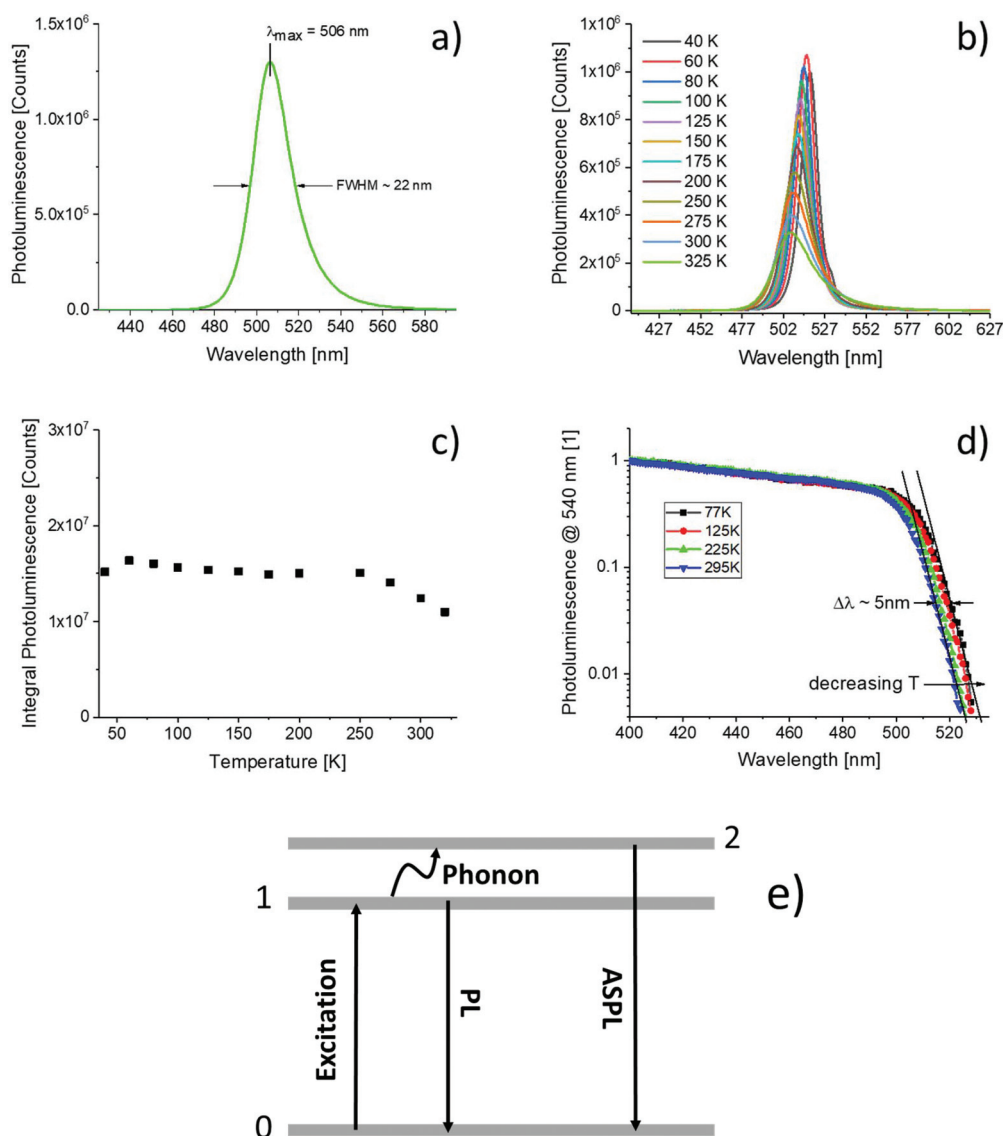
Fig. 1 (a) Photoluminescence of a thin film of $CH_3NH_3PbBr_3$ nanoparticles recorded at room temperature; (b) PL spectra of the same film recorded at different temperatures; (c) integrals of the PL-spectra plotted *versus* the temperature; (d) PL excitation spectra of the same film recorded at different temperatures; (e) energy level scheme for phonon-assisted up-conversion.

these nanocrystals are still not fully understood. Self-trapped exciton,[17] emission from trions,[18] trap assisted recombination[19] and the excited states splitting into dark and bright exciton[13,20] have been suggested to explain the temperature dependence and the decay kinetics of the observed photoluminescence.

Here, we study the anti-Stokes photoluminescence of thin films of methylammonium lead bromide ($CH_3NH_3PbBr_3$) colloidal nanoparticles with a size of about 7 nm. As the Bohr radius of the exciton is smaller compared to the particle size, the exciton is weakly confined.[21] Temperature dependent Stokes and anti-Stokes photoluminescence and photoluminescence excitation spectra are recorded and the anti-Stokes quantum efficiency (η_{ASPL}) is estimated as a function of the sample temperature. We find that η_{ASPL} strongly depends on the temperature and decreases by a factor of 50 when cooled from room temperature to 100 K.

Experimental

Chemicals

Lead(II) bromide ($PbBr_2$; 99.999%) was purchased from Sigma-Aldrich. Methylammonium bromide (MABr) was purchased from GreatCell. *t*-Boc-L-lysine (97%) was purchased from Alfa Aesar. Hexanoic acid (HeA; 98%) was purchased from TCI. Anhydrous *N,N*-dimethylformamide (DMF) was purchased from Sigma-Aldrich. Toluene of reagent grade (≥99.8%) was purchased from VWR and used as received.

Film preparation

The nanoparticles were prepared following the procedure described in ref. 22. Briefly, methylammonium lead bromide nanoparticles were prepared by ligand assisted precipitation in toluene using *tert*-butoxycarbonyl-lysine and hexanoic acid as ligands. 32 mol equivalents of water were used as an additive to the precursor solution to control the complex formation and growth of the perovskite nanoparticles. After isolation and several washing steps, thin films were prepared by depositing the nanoparticles onto glass substrates (1 × 1 cm) using centrifugal casting (at 5000 rpm for 10 minutes), and consequently dried under toluene atmosphere.

Characterization methods

Photoluminescence and excitation spectra were recorded with a standard photoluminescence spectrometer (QuantaMaster 40 (PTI)) equipped with a liquid nitrogen cryostat (Oxford OptistatDN). Low temperature and anti-Stokes photoluminescence was measured using a home-built setup. Samples were mounted on a cold finger of a closed cycle helium cryostat (Oxford OptistatDry) or in a Quantum Design Physical Properties Measurement System (PPMS). For photoluminescence measurements, samples were excited by Coherent OBIS Lasers 405 nm LX. For anti-Stokes photoluminescence measurements an OBIS 532 nm LS was used. The diameters of the laser spots on the sample were 2 mm for

the 405 nm and 3 mm for the 532 nm laser. The sample emission was collected using an optical fiber arrangement and fed into a monochromator (Shamrock 303i, grating 500 nm blaze, 150 lines per mm) and detected with an intensified charge-coupled device (Andor, iStar A-DH320T-18U-73). A long-pass filter (420 nm) was used for photoluminescence experiments. An additional notch filter (532 nm, Thorlabs) was applied for the anti-Stokes photoluminescence measurements. The absolute PL quantum yield of the investigated films was measured using a Hamamatsu C9920-03 spectrometer with an integrating sphere.

Results and discussion

The surface roughness of the resulting films was very high and all films exhibited strong light scattering. Fig. 1(a) shows the photoluminescence of a thin film of $CH_3NH_3PbBr_3$ nanoparticles on a glass substrate recorded at room temperature. The sample was excited by monochromatic light (405 nm) and the spectrum is corrected for the response of the spectrometer. The observed emission spectrum is slightly asymmetric with a maximum at 506 nm. The full width half maximum (FWHM) of the line is approximately 22 nm. The photoluminescence quantum yield of the thin film of nanoparticles was found to be 75 ± 5% when excited at 405 nm. In Fig. 1(b), the temperature dependence of the photoluminescence of the investigated nanoparticle film is summarized. Upon decreasing the temperature, the emission maximum shifts to lower energies. The emission lines narrowed and the signal intensities increased by about 25% (Fig. 1(c)). The normalized photoluminescence excitation spectra recorded between 295 K and 77 K are shown in Fig. 1(d). For all spectra, the photoluminescence intensity at 540 nm was detected while scanning the excitation. The onset of the excitation spectrum shifts to lower wavelengths ($\Delta\lambda \sim$ 5 nm) when the temperature is reduced from 295 to 77 K (Fig. 1(d)).

Fig. 2(a) and (b) show the photoluminescence of the nanoparticles when excited at 494 nm and 514 nm respectively. For comparison, the photoluminescence recorded with 405 nm excitation scaled to fit to the low energy part of the spectra is shown as well. Both spectra contain also an additional peak from the excitation. When excited at 494 nm, the shape and position of the recorded spectrum perfectly fits to the reference spectrum. When excited at 514 nm, a red shift is observed.

The redshift of the anti-Stokes PL arises from the residual size distribution of the particle ensemble.[14] Tuning the excitation wavelength to the low energy side of the nanoparticle absorption, the excitation of larger particles is preferred leading to a red spectral shift. This idea is supported by the fact that no redshift has been observed in the anti-Stokes PL spectrum of an individual perovskite nanoparticle.[23]

Fig. 3(a) shows the temperature dependence of the photoluminescence when the film is excited with 532 nm photons. In this experiment, a notch filter is placed in front of the
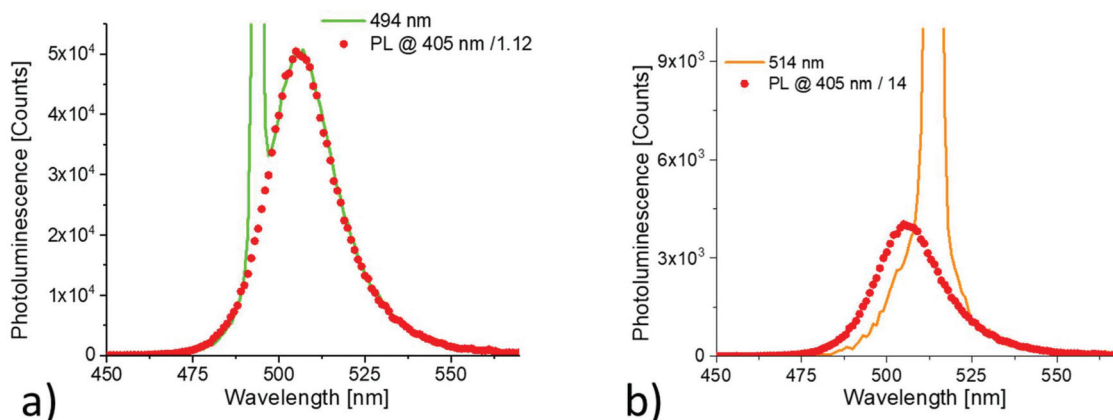
Fig. 2 Stokes and anti-Stokes PL spectra of $CH_3NH_3PbBr_3$ nanoparticle thin film recorded at room temperature; excitation: (a) 494 nm, (b) 514 nm.
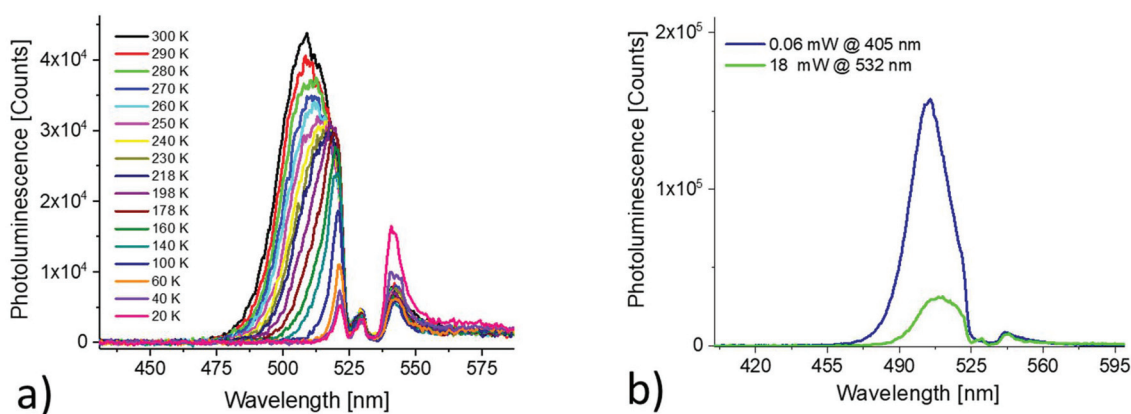

Fig. 3 (a) Anti-Stokes PL recorded at different temperatures; (b) comparison between Stokes and anti-Stokes PL spectra recorded at room temperature.

monochromator to attenuate the intense laser radiation (18 mW). The anti-Stokes PL decreases significantly upon decreasing the temperature. Under the same experimental conditions, also the Stokes PL (405 nm, 0.06 mW) was recorded on the same spot of the thin film sample. In Fig. 3(b) the Stokes and anti-Stokes PL recorded at room temperature are compared.

A strong redshift of the anti-Stokes emission is observed when excited with intense 532 nm laser light. An analysis of the Stokes and anti-stokes PL and the recorded excitation spectra allows the estimation of the anti-Stokes PL up-conversion efficiency given by equation:[23]

$$\eta_{ASPL} = \frac{N_{ASPL} \times N_{abs,405}}{N_{PL} \times N_{abs,532}}.$$

N_{ASPL} and N_{PL} correspond to the number of emitted photons when excited at 532 and 405 nm respectively. $N_{abs,405}$ and $N_{abs,532}$ correspond to the number of absorbed photons when excited at 405 and 532 nm respectively. In Fig. S1 in the ESI,† the normalized excitation spectra measured at different temperatures are shown. Several different spectra, recorded at
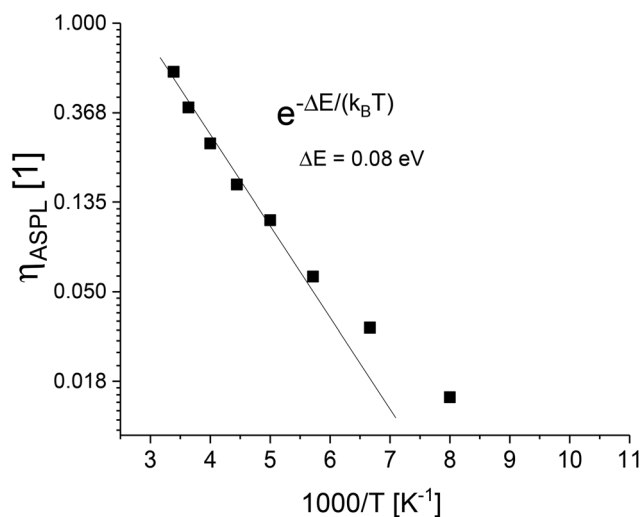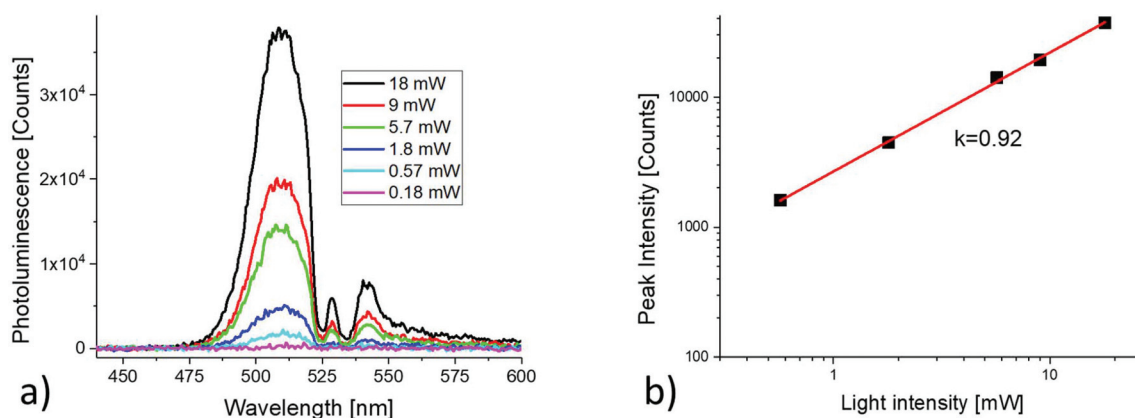

Fig. 4 Temperature dependence of the calculated anti-Stokes up-conversion efficiency.

Fig. 5 Light intensity dependence of the anti-Stokes PL. (a) ASPL spectra recorded at different light intensities; (b) log–log plot of the ASPL peak intensity *versus* light intensity.

different emission wavelengths are plotted on top of each other for each temperature. $N_{abs,532}/N_{abs,405}$ is estimated by extrapolation of the spectra to 532 nm and needs to be corrected for different laser intensities. Fig. S2† shows the temperature dependence of the ratio of absorbed photons at 405 nm and 532 nm normalized to the incoming photon flux. The red line represents a second order polynomial fit, which is used to extract data points at different temperatures between the measured data.

Fig. 4 shows the calculated anti-Stokes PL up-conversion efficiency as a function of the temperature. N_{ASPL} and N_{PL} are obtained by integration of the measured PL spectra between 450 and 518 nm. $N_{abs,405}/N_{abs,532}$ is determined as described before. At room temperature, the up-conversion efficiency is high and drops quickly upon decreasing the temperature. Between room temperature and 200 K, the up-conversion efficiency shows Arrhenius type dependence with an activation energy of 80 meV.

In Fig. 5(a), the anti-Stokes PL spectra recorded at different laser intensities are plotted. Fig. 5(b) shows the log–log plot of the anti-Stokes PL peak intensity *versus* the light intensity. The line with a slope of 0.92 is the linear fit of data points.

In this study we have demonstrated that an ensemble of $CH_3NH_3PbBr_3$ nanoparticles efficiently up-convert low energy photons. The experimental results presented above suggest that $CH_3NH_3PbBr_3$ nanocrystals are promising candidates for highly efficient anti-Stokes photoluminescence up-conversion. The anti-Stokes emission depends linearly on the excitation intensity suggesting that the underlying process is based on a one-photon mechanism. The observed temperature dependence suggests that the up-conversion process is thermally activated. Considering the moderate PLQY of the studied samples and the rather large energy difference (~100 meV) between the barycenter of the photoluminescence spectrum (~510 nm) and the photoexcitation (532 nm), the estimated ASPL conversion efficiency of ~60% is very high. However, the current particle performance is not sufficient to achieve optical cooling. Preliminary photother-

mal deflection spectroscopy (PDS) studies show a strongly distorted absorbance spectrum of the studied film due to the photoluminescence of the nanoparticles but no evidence of optical cooling. To achieve cooling, the photoluminescence quantum yield of the $CH_3NH_3PbBr_3$ nanoparticles needs to be >96% (ESI, Fig. S3†). This may be achievable by further improving the quantum dot synthesis and the film formation and by embedding the nanoparticles in an optically clear matrix for better out-coupling of the anti-Stokes photoluminescence.

Conclusions

We have studied the anti-Stokes photoluminescence properties of $CH_3NH_3PbBr_3$ nanoparticles. We find an ASPL up-conversion efficiency of approximately 60% at room temperature. The ASPL shows strong temperature dependence and a linear dependence on the light intensity. The experimental results suggest that upon improving the photoluminescence quantum yield, the studied material could be suitable for the demonstration of photon cooling.

Conflicts of interest

The authors declare no conflicts of interest.

Acknowledgements

References

1 *Halide Perovskites: Photovoltaics, Light Emitting Devices and Beyond*, ed. T.-C. Sum and N. Mathews, Wiley-VCH, 2019, ISBN: 978-3-527-34111-5.

2 S.-T. Ha, C. Shen, J. Zhang and Q. Xiong, Laser cooling of organic – inorganic lead halide perovskites, *Nat. Photonics*, 2016, **10**, 115–121.

3 B. J. Roman and M. Sheldon, The role of mid-gap states in all-inorganic CsPbBr 3 nanoparticle one photon up-conversion, *Chem. Commun.*, 2018, **54**, 6851–6854.

4 B. A. Koscher, J. K. Swabeck, N. D. Bronstein and A. P. Alivisatos, Essentially trap-free CsPbBr 3 colloidal nanocrystals by postsynthetic thiocyanate surface treatment, *J. Am. Chem. Soc.*, 2017, **139**, 6566–6569.

5 F. Liu, *et al.*, Highly luminescent phase-stable CsPbI 3 perovskite quantum dots achieving near 100% absolute photoluminescence quantum yield, *ACS Nano*, 2017, **11**, 10373–10383.

6 S.-W. Dai, *et al.*, Perovskite quantum dots with near unity solution and neat-film photoluminescent quantum yield by novel spray synthesis, *Adv. Mater.*, 2018, **30**, 1705532.

7 S. Ananthakumar and S. Moorthy Babu, Progress on synthesis and, applications of hybrid perovskite semiconductor nanomaterials—A review, *Synth. Met.*, 2018, **246**, 64–95.

8 S. A. Kulkarni, S. G. Mhaisalkar, N. Mathews and P. P. Boix, Perovskite Nanoparticles: Synthesis, Properties, and Novel Applications in Photovoltaics and LEDs, *Small Methods*, 2019, **3**, 1–16.

9 P. Pringsheim, Zwei Bemerkungen über den Unterschied von Lumineszenz- und Temperaturstrahlung, *Z. Phys.*, 1929, **57**, 739–746.

10 L. Landau, On the Thermodynamics of Photoluminescence, *J. Phys. (Moscow)*, 1946, **10**, 503–506.

11 C. W. Hoyt, M. Sheik-Bahae, R. I. Epstein, B. C. Edwards and J. E. Anderson, *Phys. Rev. Lett.*, 2000, **87**, 3600.

12 R. I. Epstein, M. I. Buchwald, B. C. Edwards, T. R. Gosnell and C. E. Mungan, *Nature*, 1995, **377**, 500.

13 Y. P. Rakovich, J. F. Donegan, M. I. Vasilevskiy and A. L. Rogach, Anti-Stokes cooling in semiconductor nanocrystal quantum dots: A feasibility study, *Phys. Status Solidi A*, 2009, **206**, 2497–2509.

14 S. Zhang, M. Zhukovskyi, B. Jankó and M. Kuno, Progress in laser cooling semiconductor nanocrystals and nanostructures, *NPG Asia Mater.*, 2019, **11**(54), 1–19.

15 J. Zhang, D. Li, R. Chen and Q. Xiong, Laser cooling of a semiconductor by 40 kelvin, *Nature*, 2013, **493**, 504–508.

16 S. T. Ha, C. Shen, J. Zhang and Q. Xiong, Laser cooling of organic-inorganic lead halide perovskites, *Nat. Photonics*, 2016, **10**, 115–121.

17 X. Ma, *et al.* Mechanism of Single-Photon Upconversion Photoluminescence in All-Inorganic Perovskite Nanocrystals: The Role of Self-Trapped Excitons, *J. Phys. Chem. Lett.*, 2019, **10**, 5989–5996.

18 M. Fu, *et al.* Neutral and Charged Exciton Fine Structure in Single Lead Halide Perovskite Nanocrystals Revealed by Magneto-optical Spectroscopy, *Nano Lett.*, 2017, **17**, 2895–2901.

19 Z.-Y. Zhang, *et al.* The Role of Trap-assisted Recombination in Luminescent Properties of Organometal Halide CH3NH3PbBr3 Perovskite Films and Quantum Dots, *Sci. Rep.*, 2016, **6**, 27286.

20 P. Tamarat, *et al.* The ground exciton state of formamidinium lead bromide perovskite nanocrystals is a singlet dark state, *Nat. Mater.*, 2019, **18**, 717–724.

21 K. Tanaka, *et al.* Comparative study on the excitons in lead-halide-based perovskite-type crystals CH3NH3PbBr3 CH3NH 3PbI3, *Solid State Commun.*, 2003, **127**, 619–623.

22 A. Jancik Prochazkova, *et al.* Controlling Quantum Confinement in Luminescent Perovskite Nanoparticles for Optoelectronic Devices by the Addition of Water, *ACS Appl. Nano Mater.*, 2020, **3**, 1242–1249.

23 Y. V. Morozov, S. Zhang, M. C. Brennan, B. Janko and M. Kuno, Photoluminescence Up-Conversion in CsPbBr3 Nanocrystals, *ACS Energy Lett.*, 2017, **2**, 2514–2515.